Journal of Nuclear Materials 398 (2010) 43–48

Contents lists available at ScienceDirect

Journal of Nuclear Materials

journal homepage: www.elsevier.com/locate/jnucmat

The microstructure and tensile properties of ferritic/martensitic steels T91, Eurofer-97 and F82H irradiated up to 20 dpa in STIP-III

Z. Tong [a,b], Y. Dai [a,*]

[a] Paul Scherrer Institute, 5232 Villigen PSI, Switzerland
[b] China Institute of Atomic Energy, 102413 Beijing, China

A B S T R A C T

Ferritic/martensitic (FM) steels, T91, Eurofer-97 and F82H, were irradiated up to a maximum displacement dose of 20 dpa (displacement per atom) at temperatures ranging from ~120 to ~600 °C in the 3rd experiment of the SINQ Target Irradiation Program (STIP-III). Tensile tests were performed at 25,400 and 450 °C. Microstructural observations show that irradiation-induced defect clusters formed in all investigated specimens, although the densities were low in specimens irradiated at temperatures >400 °C. High-density small He bubbles were observed in specimens irradiated to doses $\gtrsim$ 9 dpa. Small bubble size in specimens of high doses of 17–20 dpa at temperatures >400 °C could be attributed low temperatures in the beginning phase of irradiation. The tensile test results demonstrate that not only the specimens irradiated at <350 °C but also those irradiated at >400 °C show significant hardening effect. The three FM steels present a great similarity in tensile properties under similar irradiation and testing conditions.

1. Introduction

Ferritic/martensitic steels such as T91, F82H and Eurofer-97 have been considered as candidate structural materials for wide applications in advanced nuclear fission [1,2] and fusion [3–5] devices. All the three steels have been intensively studied in the fusion materials program because of their relatively low increase in the ductile-to-brittle-transition temperature (DBTT) after neutron irradiation. These steels are also selected as main materials irradiated and studied in the SINQ (the Swiss Spallation Source) Target Irradiation Program (STIP) [6,7] due to their promising applications in advanced high power spallation targets [8–10]. A lot of work has been done in recent years on studying the microstructure and tensile properties of these steels after irradiation (e.g. [11–16]), but mostly at low temperatures ($\lesssim$ 400 °C). In this work, the microstructure and tensile properties of these three steels irradiated in STIP-III in a temperature range of 120–600 °C to displacement doses of 6.5–20 dpa have been studied.

2. Experimental

2.1. Materials

The T91 steel was supplied by the Ugine (France) company for the EU FP5 SPIRE program. The heat number was 36224. The as-received material was in the form of a 15-mm-thick plate. The steel was normalized at 1040 °C for 1 h followed by air cooling, and then tempered at 760 °C for 1 h and followed by air cooling.

The Eurofer-97 steel (Lot 250) in the form of a 25 mm thick plate was received from Forschungszentrum Karlsruhe. The heat number was E83697. The steel was normalized at 980 °C for 27 min followed by air cooling, and tempered at 760 °C for 1.5 h and followed by air cooling.

The F82H (mod), IEA Heat 974, was obtained from the fusion materials community in the form of a 15 mm thick plate. The steel was normalized at 1040 °C for 38 min and tempered at 750 °C for 1 h.

The chemical compositions of these steels are given in Table 1. Metallography observations indicate that in the as-received T91, Eurofer-97 and F82H, the mean grain sizes are about 29 ± 6, 16 ± 2 and 86 ± 20 μm and the micro-hardness ($HV_{0.05}$) values are 258 ± 14, 237 ± 5 and 220 ± 5, respectively [17].

2.2. Irradiation

The STIP-III irradiation was effectively performed for about 68 weeks during 2002 and 2003 in SINQ target-5. As shown in [6,7] the temperature history of a STIP irradiation is usually rather complicated due to a large variation of the proton beam current (about ±15% around an averaged value) and a lot of beam trips (about 50 times per day with a duration of 1 min or longer) during two years. This results in a similar magnitude of temperature variation in the specimens, because they are mainly heated by the

* Corresponding author. Tel.: +41 56 310 4171; fax: +41 56 310 4529.
E-mail address: yong.dai@psi.ch (Y. Dai).

0022-3115/$ - see front matter © 2009 Elsevier B.V. All rights reserved.
doi:10.1016/j.jnucmat.2009.10.008

Table 1
Chemical compositions of the three tempered martensitic steels in wt.% (Fe in balance).

Steel	Cr	Ni	Mo	Mn	Ti	V	Nb	W	Ta	Cu	C	Si	P	S	B	N
T91	8.63	0.23	0.95	0.43	0.003	0.21	0.09	–	–	0.046	0.1	0.31	0.02	0.006	–	0.03
F82H (mod)	7.87	0.02	0.003	0.1	0.004	0.19	.0002	1.98	0.03	0.01	0.09	0.07	0.003	0.001	0.007	0.007
Eurofer-97	8.93	0.022	0.0015	0.47	0.009	0.20	0.002	1.07	0.14	0.003	0.12	0.060	<0.005	0.004	<0.001	0.018

Table 2
Irradiation parameters (dose, He content and temperature) and testing temperatures of the specimens.

Material	PIE	ID mark	Dose (dpa)	He (appm)	T_1[a] (°C)	T_2[b] (°C)	T_{av}[c] (°C)	T_{test} (°C)
T91	Tensile test	B32	7.7	520	197	158	185	25
		B01	8.8	615	204	163	190	25
		B21	10.9	805	340	267	315	25
		B18	15.5	1225	500	388	460	25
		B15	19.5	1645	604	467	560	25
		B02	8.8	615	213	170	200	350
		B22	7.7	520	197	158	185	400
		B03	8.8	615	192	154	180	400
		B05	13.0	995	392	306	365	450
		B08	17.4	1420	569	441	525	450
		B12	20.2	1715	604	467	560	450
	TEM	B01-L	7.4	500	140	115	130	
		B21-L	9.5	680	279	220	260	
		B18-L	13.6	1045	439	343	405	
		B18-H	17.3	1405	552	428	510	
		B15-H	20.3	1745	616	476	570	
Eurofer-97	Tensile test	C10	7.7	520	185	149	175	25
		C07	10.9	805	319	251	295	25
		C05	15.5	1225	548	425	505	25
		C12	7.7	520	185	149	175	400
		C11	7.7	520	214	171	200	450
		C19	10.9	805	352	276	325	450
		C18	15.5	1225	517	402	480	450
		C15	19.5	1645	626	484	580	450
	TEM	C10-L	6.5	415	151	123	140	
		C07-L	9.5	680	279	220	260	
		C07-H	12.6	955	405	316	375	
		C15-H	20.3	1745	638	493	590	
F82H	Tensile test	D01	8.8	615	181	146	170	25
		D04	13.0	995	328	257	305	25
		D09	17.4	1420	473	368	440	25
		D12	20.2	1715	564	437	520	25
		D02	8.8	615	208	167	195	400
		D05	13.0	995	383	299	355	450
		D08	17.4	1420	555	430	515	450
	TEM	D01-L	7.4	500	133	109	125	
		D04-L	11.2	830	267	211	250	
		D04-H	14.8	1165	388	303	360	
		D09-H	18.8	1565	518	402	480	
		D12-H	20.4	1714	575	446	530	

[a] T_1: the upper bound irradiation temperature corresponding to the upper bound beam current of about 1.25 mA at the target.
[b] T_2: the lower bound irradiation temperature corresponding to the lower bound beam current of about 0.95 mA at the target.
[c] T_{av}: the "averaged" irradiation temperature defined as temperature corresponding to the averaged beam current of about 1.15 mA.

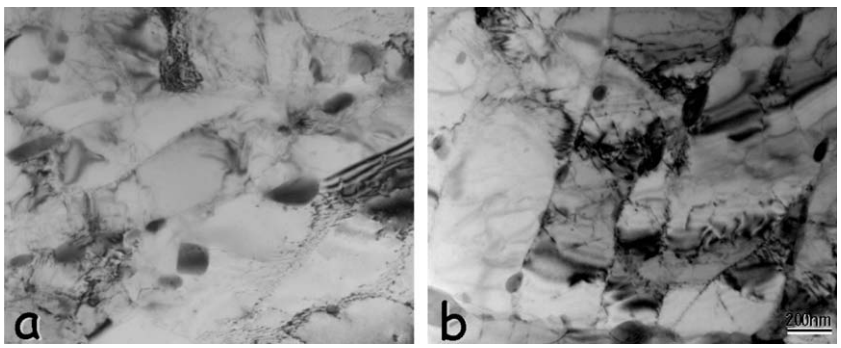

Fig. 1. BF images showing the martensitic lath structure in the T91 specimen irradiated to (a) 7.4 dpa/500 appm He at 130 °C, (b) 17.3 dpa/1405 appm He at 510 °C.

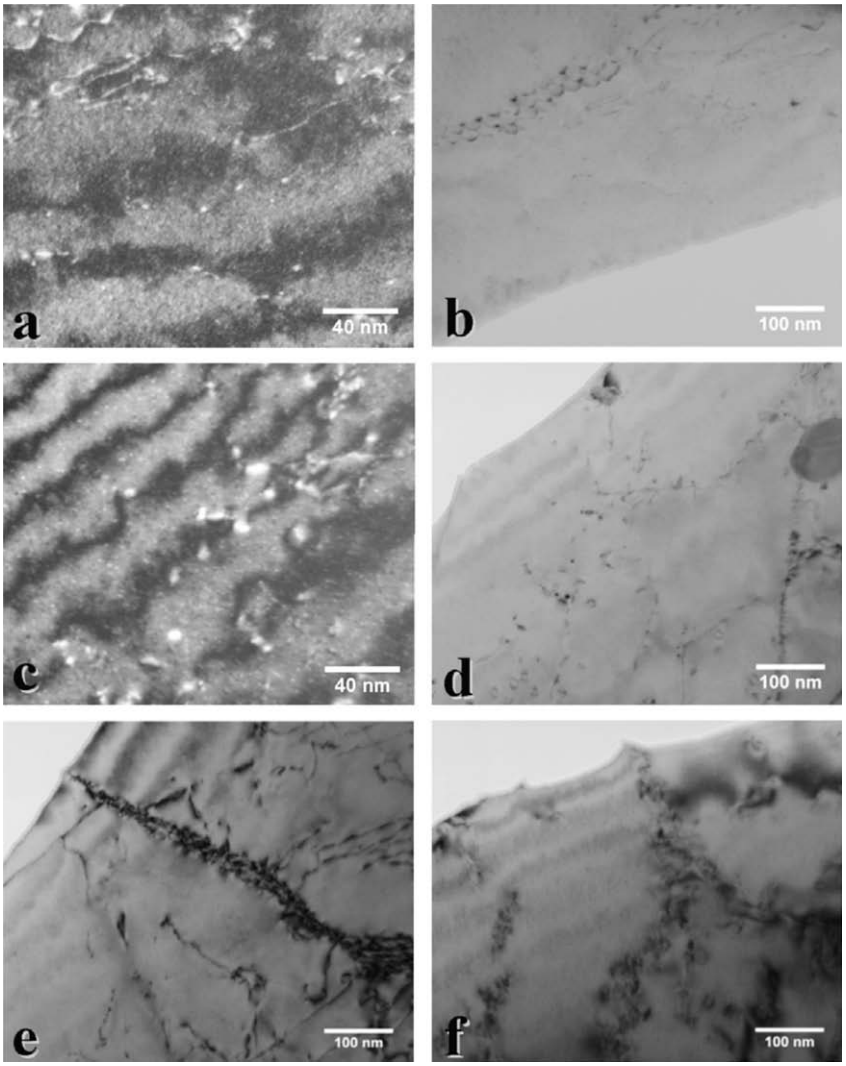

Fig. 2. WBDF (a,c) and BF (b,d,e,f) images showing the defect structure in the T91 specimen irradiated to 7.4 dpa (a and b), 13.6 dpa (c and d), 17.3 dpa (e) and 20.3 dpa (f).

proton beam. In STIP-III case, the situation was even worse. The maximum temperature of the tensile specimens used in this work was about 230 °C in the first week, and then increased to about 350 °C in the followed 7 weeks. In the 9th week, it increased greatly to about 550 °C due to a 15% increase of proton beam current and some unclear reasons. Afterwards it remained at this level or even slightly higher (~600 °C) for about 51 weeks. During the last 7 weeks of the irradiation it should decrease to about 500 °C, as the proton beam current at the target was reduced by about 20%. The temperature of each specimen was roughly proportional to the maximum value at a ratio depending on the energy deposition in the specimen. The specimens tested in this work are listed in Table 1, in which the temperature values are averaged ones calculated using the ANSYS code. As described above it should be noted that the temperature variation is about ±15%, and plus many low temperature trips.

The irradiation dose of the specimens is between 6.5 and 20 dpa and the corresponding helium concentration is between 400 and 1750 appm. The main irradiation parameters of the specimens are listed in Table 1. The hydrogen concentration of the specimens is not listed in the table, because the hydrogen content measured from steel specimens depends strongly on irradiation temperature, which can be much less than the calculated ones. Furthermore, in steel specimens irradiated at above 250 °C very little hydrogen was detected [18].

2.3. Tensile testing and TEM observation

The tensile specimens were miniature type with a gauge section of 5 mm × 1 mm × 0.4 mm, as shown in [6,7]. Tensile tests were conducted on a 2-kN MTS mechanical testing machine equipped with a video-extensometer so that the displacement could be directly measured from the gauge section. The tests were mostly conducted at room temperature (25 °C) and 450 °C at a nominal strain rate of 1×10^{-3} s^{-1}. The fracture surfaces of some specimens tested at 25 °C were observed using the scanning electron microscopy (SEM) to identify the fracture mode.

Microstructural observations were performed on specimens of 4–5 doses for each steel as listed in Table 2. Discs of 1 mm diameter were punched from the grip sections of tensile specimens after tensile testing and thinning down to about 0.2 mm. After punching, the 1.0 mm diameter discs were then embedded in 3 mm diameter discs with 1.0 mm diameter holes at the centre for electro-polishing. The observation was performed in a JEOL 2010 type transmission electron microscope (TEM) equipped with an EDX analysis system and operated at 200 keV. The most often used image conditions were bright-field (BF) and weak beam dark field (WBDF) at (**g**, **4g**) or (**g**, **5g**), **g** = **110**. Different magnifications were used depending on the objects observed. For observing small defect clusters a magnification of 200 k times or higher was applied. To obtain quantitative information, the defect clusters and Frank loops were

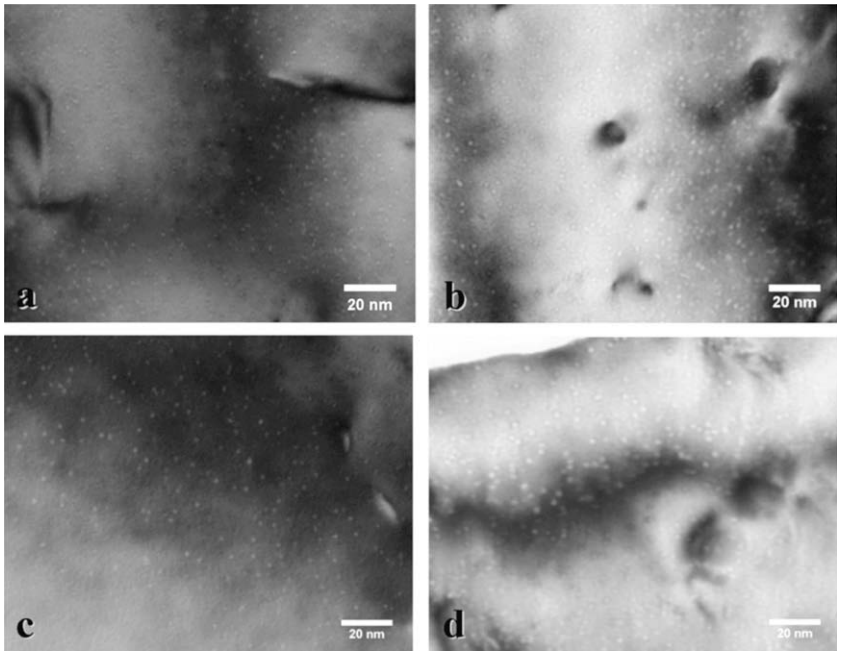

Fig. 3. BF images showing the bubble structure in the T91 specimen irradiated to (a) 9.5 dpa, (b) 13.6 dpa, (c) 17.3 dpa and (d) 20.3 dpa.

counted and measured from several pictures which were taken from different areas of each sample under the WBDF condition (**g**, **5g**).

3. Results and discussion

3.1. TEM observations

In this study, the microstructure of the three steels has been investigated in 4–5 irradiation conditions, as listed in Table 2. The microstructure of different steels has no evident difference when the specimens are in the same irradiation conditions. Therefore, in this paper the microstructure of the T91 steel is shown as a representative.

Fig. 1 presents bright-field (BF) images showing the martensitic lath structure in specimens irradiated to 7.4 and 17.3 dpa, namely the low dose and high dose conditions. It shows that the martensitic structure does not change evidently after irradiation.

The radiation-induced defect clusters and small dislocation loops were observed in all the specimens, as shown in Fig. 2. In the specimen irradiated to 7.4 dpa/500 appm He at ~130 °C, small defect clusters of 1–3 nm size, the white dots in the WBDF image (Fig. 2a), were produced by irradiation. While dislocation loops were not many. With increasing irradiation dose and temperature to 13.6 dpa/1045 appm He and 405 °C, the size and density of small loops increased (Fig. 2c and d). At irradiation temperature above 500 °C, very few clusters or loops were observed (Fig. 2e and f).

The radiation-induced He-bubble structure is illustrated in Fig. 3. In the specimen irradiated to 7.4 dpa/500 appm He at 130 °C, no bubbles could be visible with the JEOL 2010 microscope which has an effective resolution limit about 0.5–1 nm. In the other specimens, high-density small He-bubbles were observed, as shown in Fig. 3. Although a trend could be seen in Fig. 3a–d that the size of the bubbles increased with irradiation dose and temperature, the increase of bubble size was much smaller than the anticipated one. In the previous study on the specimens irradiated in STIP-II, it showed that large He-bubbles formed in specimens irradiated at above about 400 °C [19]. The main reason for lacking large He-bubbles in the specimens irradiated at even higher temperatures could be the low temperatures in the first few weeks of the irradiation. During this period, He-bubbles or He-vacancy clusters formed at a very high density due to less mobile of helium at low temperature. These very dense He-bubbles then served as sinks to the He produced afterwards and slowed down the growth of bubbles.

3.2. Tensile tests

The results of tensile tests performed at 25, and 350–450 °C are presented in Fig. 4. Results of the T91 specimens are shown in Fig. 4a and b. Tests performed at 25 °C indicate that the specimens at different doses have some differences in deformation behavior, although all of them showing significant hardening as compared to the unirradiated specimen. The specimens irradiated to lower doses $\leqslant$8.8 dpa at lower temperatures <200 °C show little or no work hardening capability, while the specimens irradiated to higher doses $\geqslant$10.9 dpa at >300 °C display obvious recovery of work hardening and uniform elongation. The tensile curves of the specimens tested at 350–450 °C (Fig. 4b) are similar to those of tests at 25 °C (Fig. 4a), although the overall strength of the specimens decreases by 200–300 MPa depending on test temperature. The specimens irradiated to lower doses $\leqslant$8.8 dpa at lower temperatures <200 °C present again prompt necking behavior, while the specimens irradiated to higher doses $\geqslant$11 dpa at >300 °C have a similar or even greater uniform elongation as compared to that of unirradiated specimens.

The results of the specimens of Eurofer-97 (Fig. 4c and d) and F82H (Fig. 4e and f) are similar to those of the T91 specimens, except that two F82H specimens of 17.4 and 20.2 dpa exhibit a very brittle failure without any plastic deformation for testing at 25 °C.

The fracture surfaces of some tensile tested specimens were observed using SEM. Except for the two F82H specimens breaking in the elastic regime, all other specimens broke in a ductile and transgranular fracture mode. The two F82H specimens of 17.4 and 20.2 dpa tested at 25 °C broke in a brittle manner with mostly intergranular appearance on fracture surfaces as shown in Fig. 2

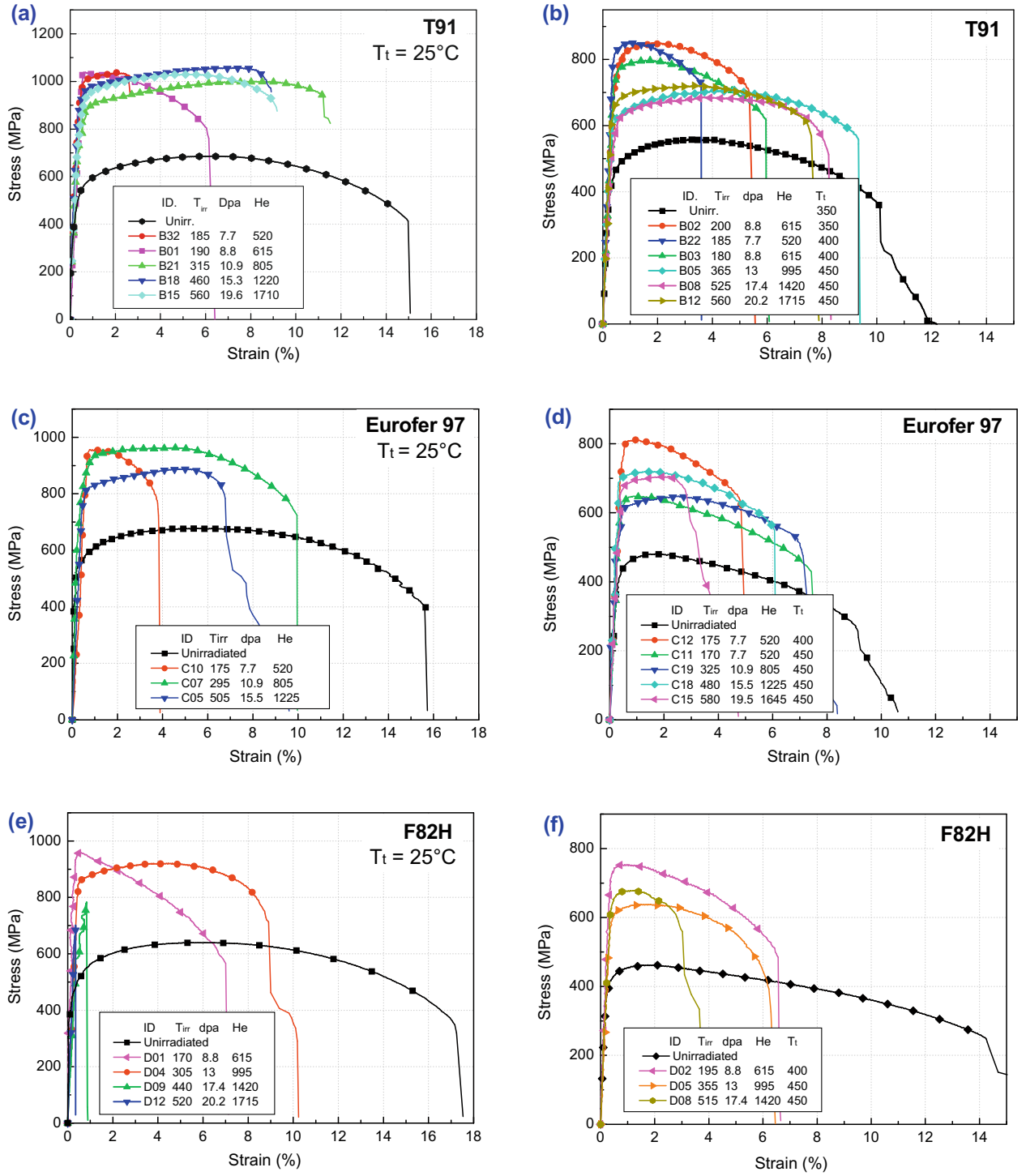

Fig. 4. Tensile stress–strain curves of the specimens of T91, Eurofer-97 and F82H irradiated in STIP-III and tested at 25 °C, and 350–450 °C. The unit for the He concentration is appm and for the temperature is degree Celsius.

of [20]. The difference in the fracture or tensile behaviors of the two high-dose F82H specimens as compared to that the T91 or Eurofer-97 ones is not well understood. One possible reason could be that the grain size of F82H is much larger than that of T91 or Eurofer-97 (see Section 2.1).

In the previous work [16], tensile tests on FM steels irradiated in STIP-I to doses up to ~12 dpa at $\leqslant$370 °C do not show evident differences. The tensile properties of the three kinds of steels irradiated to higher doses and at higher temperatures have a general similarity. Nevertheless, it looks the T91 steel has greater ductility at high doses as compared to the Eurofer-97 and F82H steels in similar irradiation and test conditions.

As discussed in the previous work on the results of the F82H steel [20], the hardening of specimens irradiated at $\gtrsim$ 450 °C may be mainly attributed to high-density He-bubbles. The results of the T91 and Eurofer-97 steels obtained in this work confirm this observation. A more detailed analysis of He-bubbles induced hardening will be reported in the future.

4. Conclusions

Three FM steels, T91, Eurofer-97 and F82H, were irradiated in STIP-III (SINQ Target-5) to doses between 6.5 and 20.4 dpa at temperatures ranging from ~120 to ~600 °C. Tensile tests were conducted at 25, 350, 400 and 450 °C. TEM observations were performed on ϕ1 mm discs punched from the grip sections of the tensile specimens tested at 25 °C. The main conclusions drawn from the results are as the following:

(i) Radiation-induced defect clusters and small dislocation loops were observed in specimens irradiated to lower doses at lower temperatures. In specimens irradiated at temperatures $\gtrsim$ 400 °C, much less clusters or loops were observed. He-bubbles were seen in specimens irradiated to $\geqslant$9.5 dpa/680 appm He at $\geqslant$260 °C. But the size of the bubbles did not increase so much with increasing irradiation dose as observed in the previous work [19], which should be attributed to the high-density bubbles nucleated at low temperatures during the first irradiation period.

(ii) Not only the specimens irradiated at lower temperatures $\lesssim$ 350 °C, but also those irradiated at higher temperatures above >400 °C show a significant hardening effect. The hardening observed in these specimens should be attributed to the hardening effect of He-bubbles.

(iii) The three FM steels show a general similarity in tensile properties in similar irradiation and testing conditions, except for the brittle fracture observed from two F82H specimens of 17.4 and 20.2 dpa tested at 25 °C, which was not detected for the T91 and Eurofer-97 steels.

Acknowledgement

The authors would like to thank Mr. R. Brun and the operators of the hot-cell group of PSI for their help. The present study is partly supported by EU FP6 EUROTRANS Program under contract: FI6W-CT-2004-516520.

References

[1] R.L. Klueh, A.T. Nelson, J. Nucl. Mater. 371 (2007) 37.
[2] C. Fazio, A. Alamo, A. Almazouzi, S. De Grandis, D. Gomez-Briceno, J. Henry, L. Malerba, M. Rieth, J. Nucl. Mater. 392 (2009) 316.
[3] S. Jitsukawa, A. Kimura, A. Kohyama, R.L. Klueh, A.A. Tavassoli, B. van der Schaaf, G.R. Odette, J.W. Rensman, M. Victoria, C. Petersen, J. Nucl. Mater. 329–333 (2004) 39.
[4] S.N. Rosenwasser, P. Miller, J.A. Dalessandro, J.M. Rawls, W.E. Toffolo, W. Chen, J. Nucl. Mater. 85&86 (1979) 177.
[5] A. Kohyama, A. Hishinuma, D.S. Gelles, R.L. Klueh, W. Dietz, K. Ehrlich, J. Nucl. Mater. 233–237 (1996) 138.
[6] Y. Dai, G.S. Bauer, J. Nucl. Mater. 296 (2001) 43.
[7] Y. Dai, X. Jia, R. Thermer, D. Hamaguchi, K. Geissmann, E. Lehmann, H.P. Linder, M. James, F. Gröschel, W. Wagner, G.S. Bauer, J. Nucl. Mater. 343 (2005) 33.
[8] Y. Dai, in: Proceedings of ICANS-XIII and ESS-PM4, October 11–19, 1995, PSI, p. 604.
[9] G.S. Bauer, M. Salvatores, G. Heusener, J. Nucl. Mater. 296 (2001) 17.
[10] E.J. Pitcher, J. Nucl. Mater. 377 (2008) 17.
[11] K. Shiba, R.L. Klueh, Y. Miwa, J.P. Robertson, A. Hishinuma, J. Nucl. Mater. 283–287 (2000) 358.
[12] R. Schaublin, M. Victoria, J. Nucl. Mater. 283–287 (2000) 339.
[13] Y. Dai, S.A. Maloy, G.S. Bauer, W.F. Sommer, J. Nucl. Mater. 283–287 (2000) 513.
[14] X. Jia, Y. Dai, J. Nucl. Mater. 356 (2006) 50.
[15] N. Okubo, E. Wakai, T. Tomita, S. Jitsukawa, J. Nucl. Mater. 367–370 (2007) 112.
[16] Y. Dai, B. Long, Z.F. Tong, J. Nucl. Mater. 377 (2008) 115.
[17] H. Zhang, B. Long, Y. Dai, J. Nucl. Mater. 377 (2008) 122.
[18] Y. Dai, Y. Foucher, M. James, B. Oliver, J. Nucl. Mater. 318 (2003) 167.
[19] X. Jia, Y. Dai, J. Nucl. Mater. 356 (2006) 105.
[20] Z. Tong, Y. Dai, J. Nucl. Mater. 385 (2009) 258.